SINGLE PION PRODUCTION BY HIGH-ENERGY NEUTRINOS

C. Franzinetti

Istituto di Fisica Superiore, Università di Torino
Istituto di Fisica Nucleare, Sezione di Torino

1. INTRODUCTION

In this report some of the results are presented which were obtained at Cern from the exposure of the Heavy Liquid Bubble Chamber last year to the neutrino beam.

Although the analysis of the events has now been completed, the experimental data discussed here are still those presented at Vienna Conference[1].

However, the comparison between theoretical prediction is carried out in greater detail than done in the above quoted report. Also, an estimate of the axial form factor is given, which was not attempted before.

2. DETAILS OF THE EXPERIMENTAL APPARATUS

The scheme of the experimental apparatus is shown in Fig. 1. The accelerated proton beam was extracted from the PS ring and directed towards a target. Pions and kaons, generated in the interactions produced by the proton beam, were focused towards the bubble chamber (HLBC) by a system of focusing devices indicated in the figure by the letters R1, R2 and R3. R1 is usually known as the Van der Meer horn and R2 and R3 as the Asner-Iselin reflectors. They are all described in well-known reports[3,4] and we shall not discuss them here.

Pions or kaons decaying in the space between R1 and the end of the tunnel provided the neutrino beam used in the experiment. All ionizing or strongly interacting particles were removed from the beam by a heavy shielding of 6000 t of steel, forming a thickness of 19 m. The total length of decay path, from R1 to the end of the tunnel was 57 m.

The primary proton beam impinging on the target was monitored[5] by an induction transformer, to an accuracy of $\sim$ 2%. Also the number of protons impinging on the target was measured from the radioactivity induced on aluminium foils, due to the formation of ^{22}Na of 2.6 years half-life.

The flux of muons inside the shielding, as a function of the depth, was also measured. A system of ionization chambers, scintillation counters and emulsions was used to measure the muon spectrum up to over 15 GeV/c. The knowledge of the muon spectrum gives a direct way of calibrating the neutrino flux, both in intensity and spectrum.

The HLBC--enlarged to a useful volume of $\sim$ 1000 l of which 508 l were used for the anlysis of the events -- was filled with propane (C_3H_8).

3. EXPOSURE AND ANALYSIS OF THE EVENTS

The bubble chamber was exposed for 1.08×10^6 pulses corresponding to 6.8×10^{17} protons impinging on the target.

The shape of the neutrino spectrum and the total flux of neutrinos were calculated[+] from available data on pion and kaon production. The result (see Fig. 2) was found consistent with the measurements of the muon flux obtained as described in the previous section. Due to several possible source of error which have not yet been sufficiently studied or understood, the uncertainty on each individual point of the spectrum is $\pm$ 15%.

Events produced by a neutral radiation with at least one non-interacting negative particle were selected as "neutrino-candidates". To reduce the background of events due to neutrons and to entering pions, simulating

---

+) The final spectrum is a result of a joint effort by H. Wachsmuth[6], W. Venus (unpublished), B. Pattison, D. Rusch and T. Jones (unpublished).

genuine neutrino events, it was also required that the total visible energy $E_{vis} > 0.3$ GeV and the component of the "visible momentum" parallel to the neutrino direction be $P_x > 0.3$ GeV/c.

4. SINGLE PION PRODUCTION

4.1 Experimental results

Let us consider the reactions

$$\nu + p \longrightarrow \mu^- + \pi^+ + p \qquad (4.1)$$

$$\nu + n \longrightarrow \mu^- + \pi^+ + n \qquad (4.2)$$

$$\nu + n \longrightarrow \mu^- + \pi^0 + p \qquad (4.3)$$

These are the only possible processes, induced by neutrinos on nucleons, in which only one pion is produced. Process (4.1) is the easiest to study because all its final products are charged. It is also the most frequent of the three, in a region dominated by the T=3/2 isospin state.Moreover, due to the present hydrogen in a propane molecule (C_3H_8) it occurs on a free proton in 8/26=31% of the observed cases. Events on free protons are particularly interesting because their final products are not distorted by nuclear effects.

For the same reason as above, process (4.2) is rare ($\sim$ 7.5% of the total π^+ production in C_3H_8). Process (4.3) is also comparatively rare ($\sim$ 15% of the total π^+production) and very difficult to detect. In fact using propane in the CERN HLBC the probability of detecting at least one of the two γ's from the π^0 is only $\sim$ 35%.When none of the γ's is seen,such an events would appear as an elastic process and some of them would be kinematically consistent with such an hypothesis. Thus, for the moment, we shall not consider processes (4.2) and (4.3) worth studying.

Ninety-three events were selected[1)], which were consistent with being due to process (4.1). Twelve of these contained a positive track which interacted after a short path and could not be measured precisely

or be identified with certainty. These events were disregarded and the final distribution was corrected to take into account this kind of loss.

Events on hydrogen were selected on the basis of energy and momentum balance. Since the "free" proton target is at rest in the laboratory system, the resultant momentum of the final product must be exactly in the direction of the incoming neutrino and equal to the neutrino energy. Thus the two quantities

$$P_T \text{ and } P_{x\ unb} = E_{vis} - P_{xf}$$

(P_T = component of the final momentum perpendicular to the neutrino direction; P_{xf} = component of the final momentum parallel to the neutrino direction) must be zero.

The values of P_T and $P_{x\ unb}$, for the 93-12=81 events mentioned above, are shown in Fig. 3. The condensation near the origin is interpreted as being due to events in hydrogen. The dotted square indicates the limits of our measurement errors: thus only the 49 events inside the square were taken as events of free protons. It was estimated see Ref. (1) that this sample contained $\sim$ 7 events in carbon, i.e. $\sim$ 15% of its events were on bound protons.

Taking into account all kinds of losses (unmeasurable events, background of events on carbon, scanning efficiency, measurement errors) the cross-section was calculated. The results are shown in Figs. 4, 5 and 6.

4.2 The theory of single pion production by neutrinos has been studied by several authors[7]. Many of the published calculations have been carried out using similar methods and-in most cases-produced similar results.

To discuss our experimental data, we have considered only recent papers which have included numerical predictions or expressions which give an easy access to direct numerical computations:

i) Salin's work[8]. This author assumes that the hadronic current is well approximated by the four graphs of Fig. 7. He deduces the vector

coupling from previous work on photo and electroproduction[9]; for the axial vector coupling (at $q^2=0$) he relies on dispersion relations and the static theory of Chew Goldberger Low Nambu. The q^2-dependence of the form factors is described by empirical parametric formulas which will be mentioned later.

ii) Adler's calculations[10]. These are based entirely upon the use of dispersion relations. He assumes that only those multipoles should be retained which excite the 33-resonance. The also develops on a similar method the theory of photo and electroproduction and finds his predictions in reasonably good agreement with experiments(*).

iii) A number of papers[12,13,14] where the production of the N^*_{33}-resonance is calculated by using the predictions of postulated symmetries.

Numerical values for the cross sections, calculated by these authors (or using their theory) are shown in Fig. 8.

For all of them the vector part is computed taking the vector form factor equal to the isovector electromagnetic nucleon form factors

$$F^{I.V.}_{e.m.} = \left(1 + \frac{q^2}{M_V^2}\right)^{-2} \qquad (4.4)$$

with $M_V \sim 0.85$ GeV/c^2. The axial form factors are also taken of the same form

$$F_A = \left(1 + \frac{q^2}{M_A^2}\right)^{-2} \qquad (4.5)$$

with M_A as indicated near each curve. As one can see, Adler's results differ by more than a factor 2 from most of the others. In particular, he predicts a relative ratio of the cross sections for the three reactions (4.1), (4.2), (4.3) which is $\sigma_1 : \sigma_2 : \sigma_3 =$ 3.6:1:1.3 whereas

(*) However, recent experiments at SLAC have produced experimental data which indicate a cross section for electroproduction of the 33-resonance higher than Adler's theory predicts[11].

Salin's is farly close to the ratios 9:1:2 which is to be expected for a pure $I = \frac{3}{2}$ isospin channel. Unfortunately, so far these ratios have not been accessible for a direct experimental cheek due to the fact that the average potential path of a γ-ray in the propane filled CERN chamber was less than half of the conversion mean free path.

4.4 Comparison between theory & experiments.

On this report i shall use the theory of Salin who has published his work in great detail and has also made available to us his computer program.

The curves which are drawn in Fig.s 4, 5 6 differ from those originally calculated by Salin only in the formula chosen to express the form factors. We have used the parametrix expressions (4.4) and (4.5).

Fig. 5 shows the q^2-distribution of the events integrated over the neutrino spectrum. The theoretical curves are normalized to the same number of experimental data. Figure 6 shows the missing-mass distribution of the events, i.e. dN/dM^{*2} also integrated over the spectrum and normalized to the experimental data. The quantity M^{*2} is defined as

$$M^{*2} = -(p_\nu - p_\ell + P_1)^2 \qquad (4.6)$$

where p_ν , p_ℓ and P_1 are the four-momenta of the neutrino, of the charged lepton and of the target proton respectively. If our interpretation of the event is correct, such a quantity should equal to

$$M_\beta^2 = -(P_2 + k)^2$$

In Fig. 9 the function $\Delta = (M^{*2} - M_\beta^2)/M^{*2}$ is plotted for events attributed to interactions on free protons for different cuts in P_T and $P_{x\ umb}$. The agreement between the M_β and M^* determinations is seen to be good.

By fitting our data over the theoretical curves we obtain the following "best fitting" values:

- for channel (4.1) $M_A = 1.250 \pm 0.350$ Gev/c^2
- for all channels (4.1) to (4.3) $M_A = 0.850 \pm 0.250$ Gev/c^2

If the alternative parametric form of the form factors is used

$$F_V^{Mag} = \frac{1.064}{1 + q^2/18\, m_\pi^2} - 0.064$$

$$F_V^{ch} = \frac{1.191}{1 + q^2/18\, m_\pi^2} - 0.191$$

$$F_A = \frac{1.064}{1 + q^2/M_A^2} - 0.064$$

then the following values are obtained

- for channel (4.1) $M_A = 0.850 \pm 0.250$ Gev/c^2
- for all channels (4.1) to (4.3) $M_A = 0.58 \pm 0.150$ Gev/c^2

The last value can be compared directly with that obtained from the analysis of events in freon[15]: it is in fact in very good agreement. All the values of M_A related to channel (4.1) are considerably greater than the others but not consistent with them, considering the large errors involved.

*

* *

REFERENCES

1) I. Budagov, D.C. Cundy, C. Franzinetti, W.B. Fretter, H.W.K. Hopkins, C. Manfredotti, G. Myatt, F.A. Nezrick, M. Nikolic, T.B. Novey, R.B. Palmer, J.B.M. Pattison, D.H. Perkins, C.A. Ramm, B. Roe, R. Stump, W. Venus, H.W. Wachsmuth and H. Yoshiki, contribution to the 14th International Conference on High Energy Physics, Vienna, 1968.

2) S. Bonetti, E. Fiorini, M. Rollier, J. Colas, J.L. Masnou, J. Six, I. Budagov, D.C. Cundy, C. Franzinetti, W.B. Fretter, H.W.K. Hopkins, C. Manfredotti, G. Myatt, F.A. Nezrick, M. Nikolic, T.B. Novey, R.B. Palmer, J.B.M. Pattison, D.H. Perkins, C.A. Ramm, B. Roe, R. Stump, W. Venus, H.W. Wachsmuth and H. Yoshiki, contribution to the 14th International Conference on High Energy Physics, Vienna, 1968.

3) S. Van der Meer, CERN 61-7 (1961).

4) A. Asner and Ch. Iselin, CERN 65-17 (1965).

5) H. Wachsmuth, Neutrino beam monitoring, Symposium on Beam Intensity Measurements, Daresbury, April 1968; and also, CERN Internal Report NPA/Int. 68-11 (1968).

6) H. Wachsmuth, CERN Internal Report NPA/Int. 68-20 (1968).

7) For a list of references on this subject, complete up to 1966, see C. Franzinetti, CERN 66-13 (1966).

8) Ph. Salin, Nuovo Cimento 48, 506 (1967).

9) M. Gourdin and PH. Salin, Nuovo Cimento 27, 193, 309 (1963).

10) S.L. Adler, Thesis, Princeton (1964); and Annals of Physics 1968 (in press).

11) W.K.H. Panofsky, Vienna Conference 1968, p. 35.

12) I.J. Ketley, Phys. Letters 16, 340 (1965).

13) C.H. Albright and L.S. Liu, Phys. Rev. 140B, 1611 (1965).

14) G. Altarelli, R. Gatto and G. Preparata, Nuovo Cimento 37, 1817 (1965).

15) J. Bartley, C. Franzinetti, M. Paty and Ph. Salin, CERN Internal Report NPA/Int. 65-11.

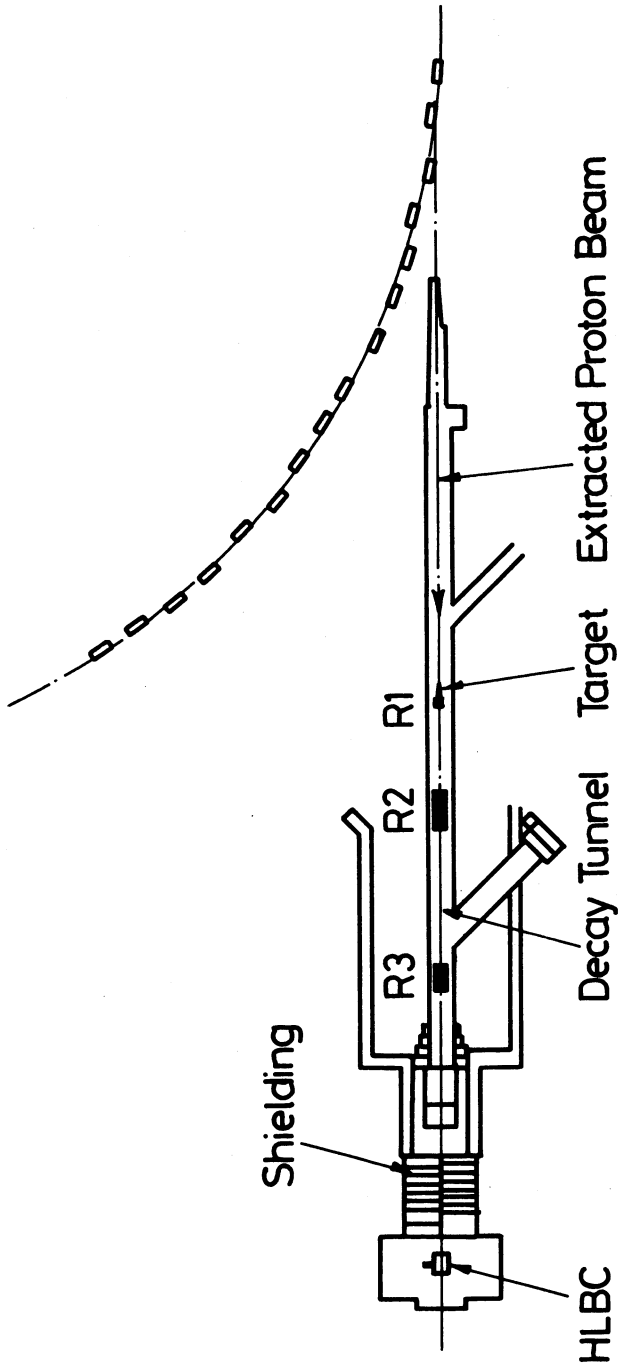

Fig. 1 : Experimental layout [deduced from Ref. (6)].

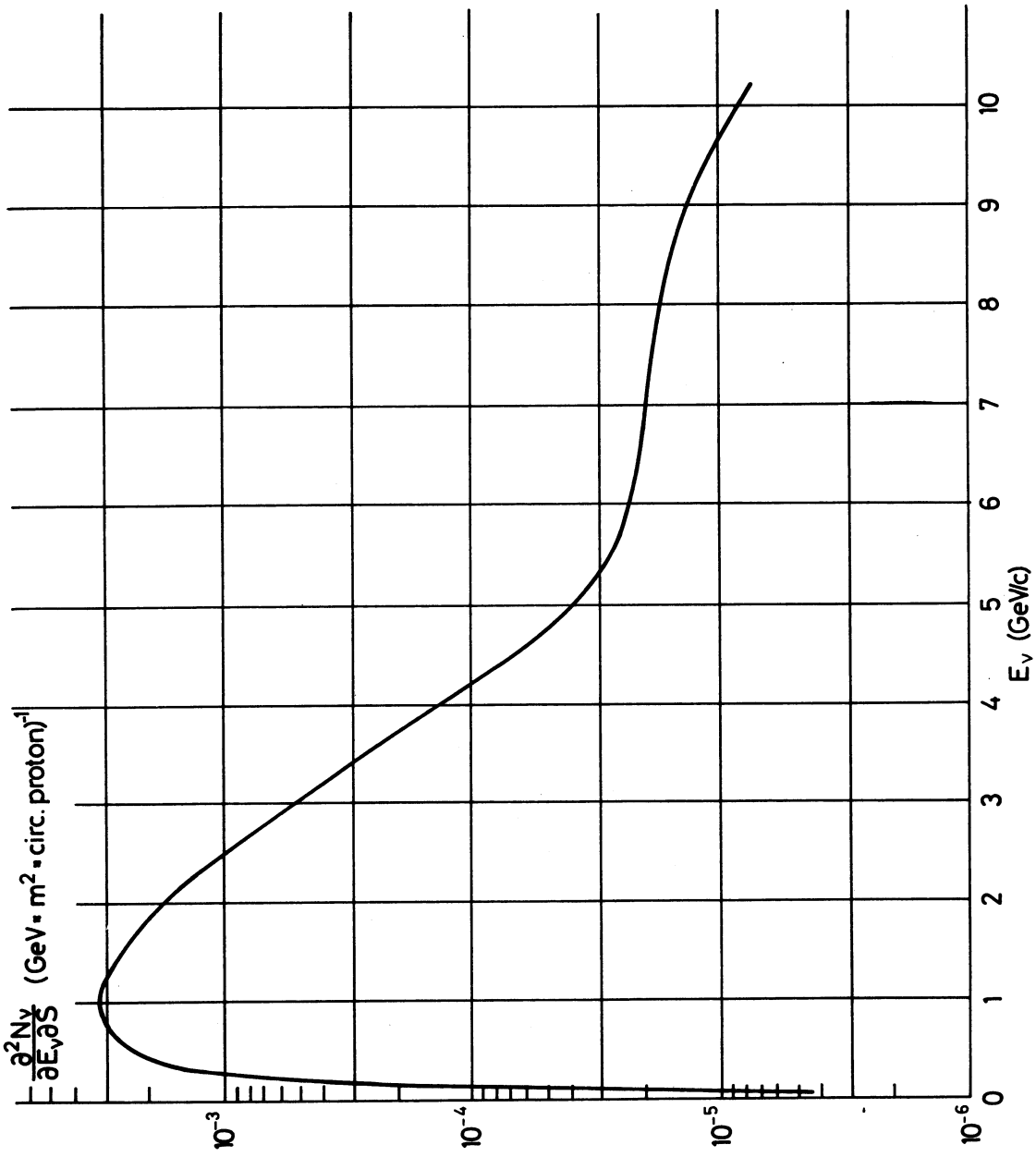

Fig. 2 : Energy distribution of neutrinos in the CERN neutrino beam used in this experiment.

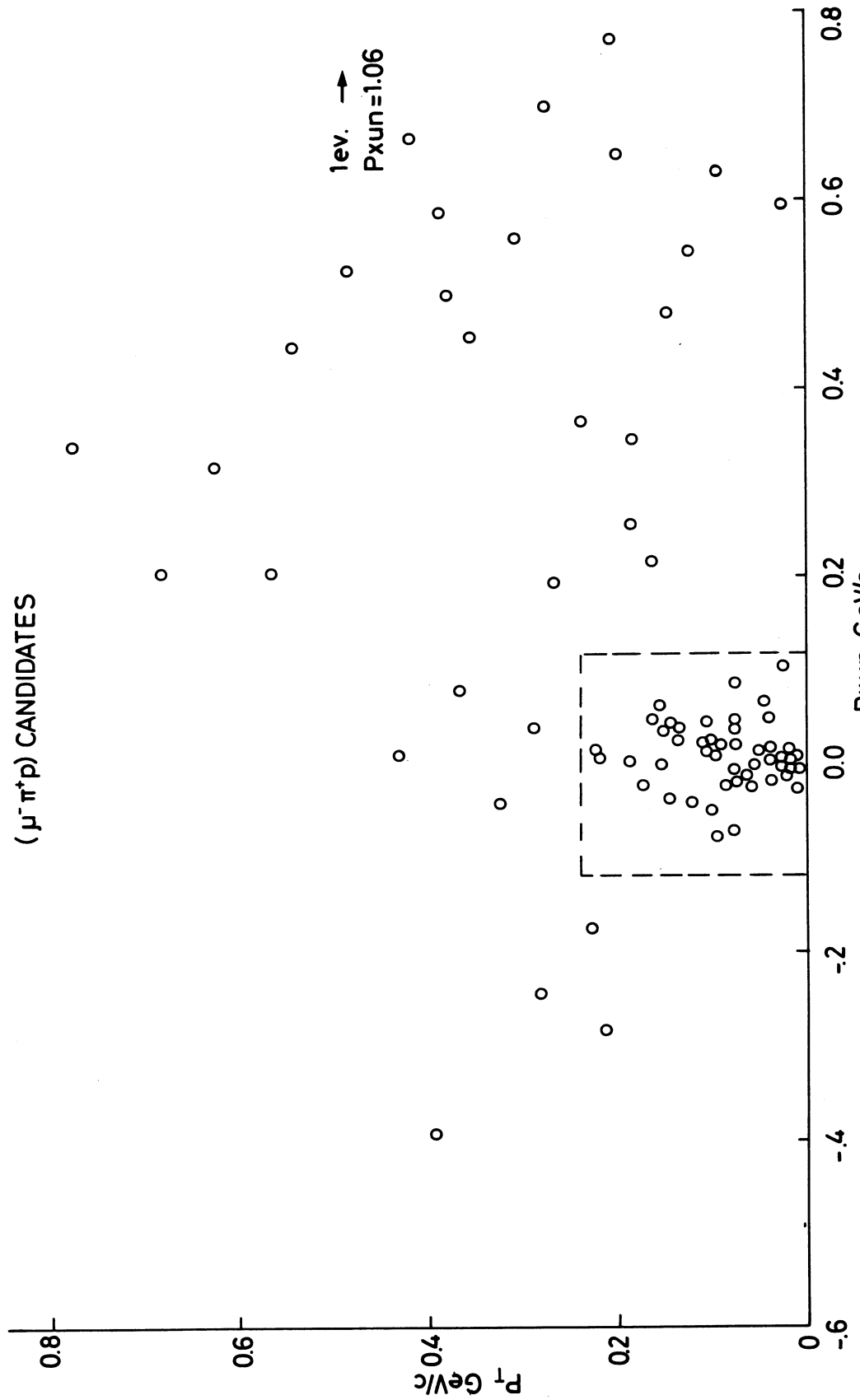

Fig. 3 : P_T versus $P_{x\ umb}$ scatter diagram for events due to the reaction
$\nu + p \rightarrow \mu^- + p + \pi^+$.

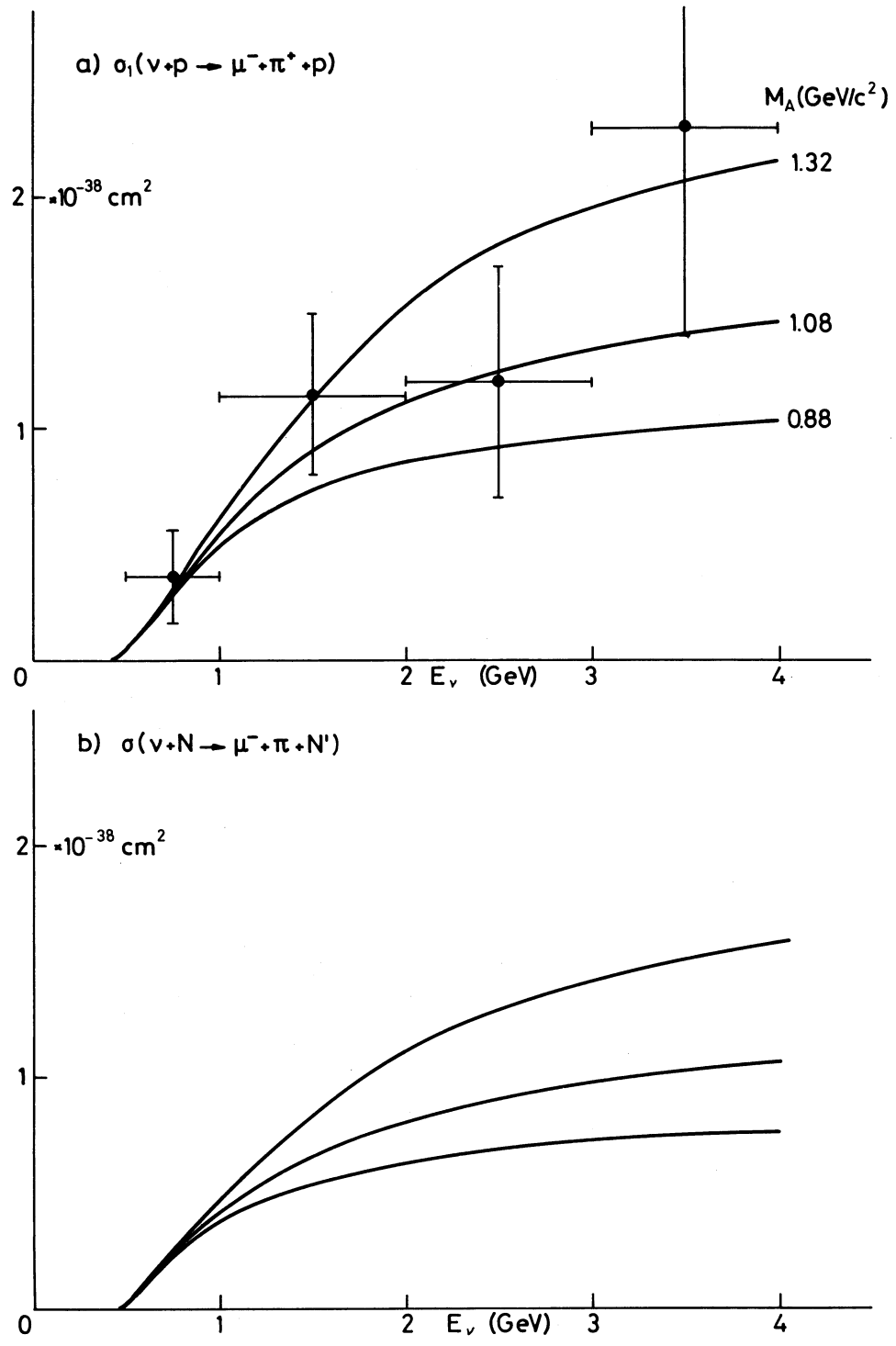

Fig. 4 : Experimental values of the cross-section for the process

a) $\nu + p \rightarrow \mu^- + p + \pi^+$

on free protons compared with the curves predicted by Salin's theory for different axial vector form factors (see text); and for

b) $\nu + N \rightarrow \mu^- + N' + \pi$

mediated over the proton neutron proportion in C_3H_8.

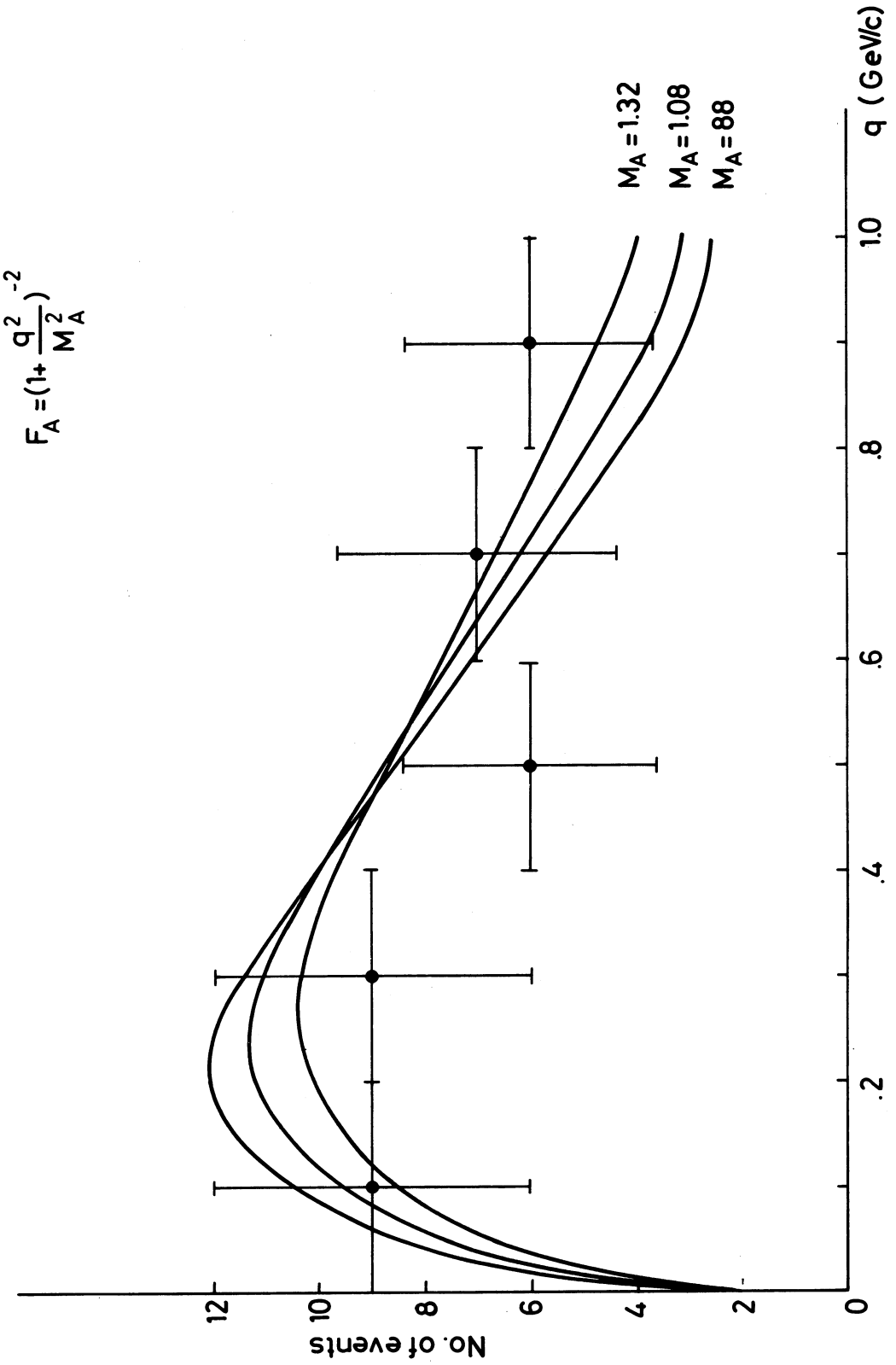

Fig. 5 : Observed q^2 distribution for the reaction $\nu + p \rightarrow \mu^- + p + \pi^+$ on free protons, compared with the curves predicted by Salin's theory for different axial vector form factors (see text).

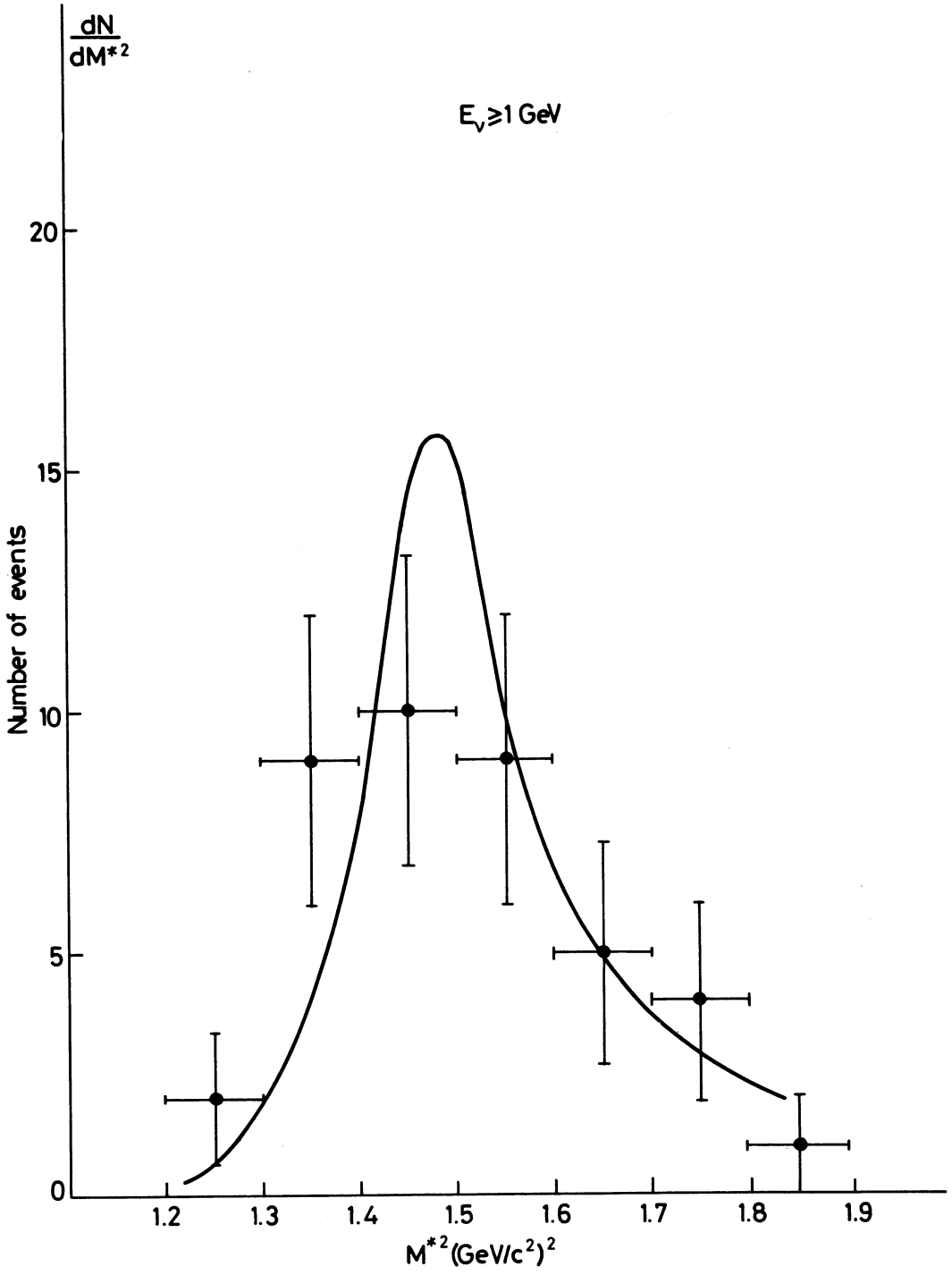

Fig. 6 : Observed M^{*2} distribution for the reaction $\nu + p \rightarrow \mu^- + p + \pi^+$ on free protons, compared with the distribution predicted by Salin's theory. This distribution depends very little on the choice of the form factors.

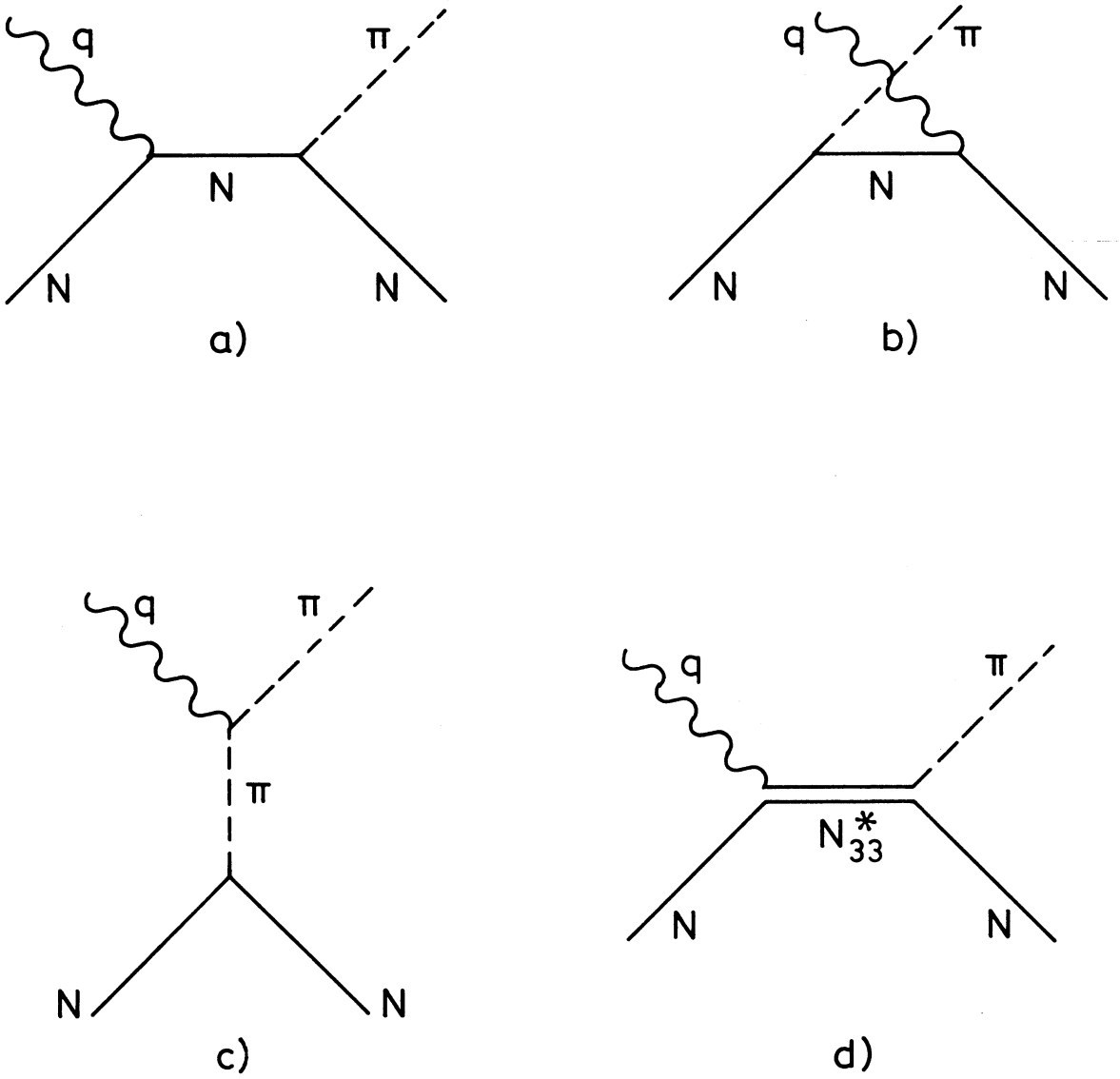

Fig. 7 : Feynman graphs used by Salin to calculate 1π -weak production.

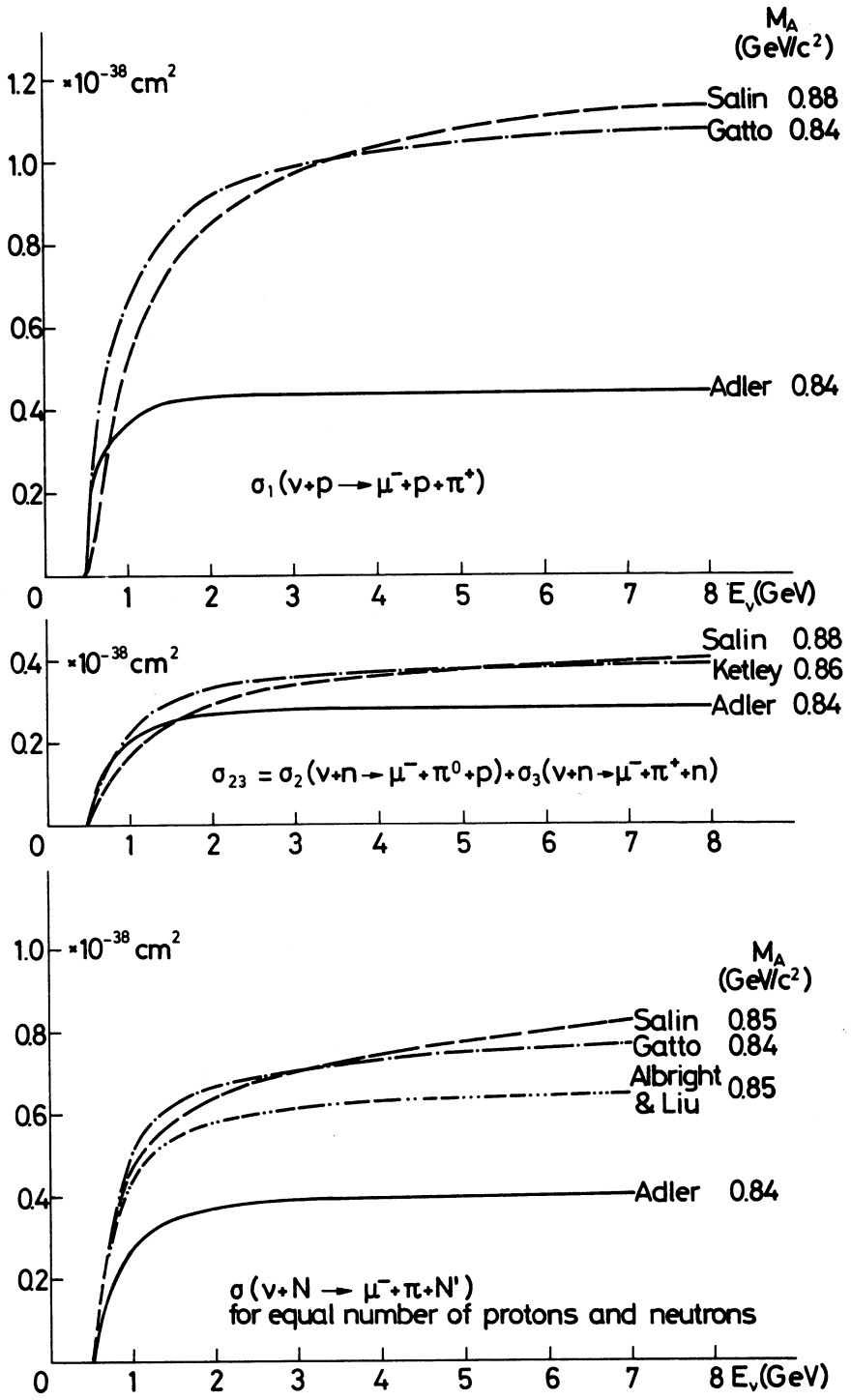

Fig. 8 : Comparison of the theoretical results obtained by different authors for different channels. The value of M_A used in each case is indicated on the right-hand side. The vector form factors are taken as equal to the **e**.m. form factors. The references are given in the text.

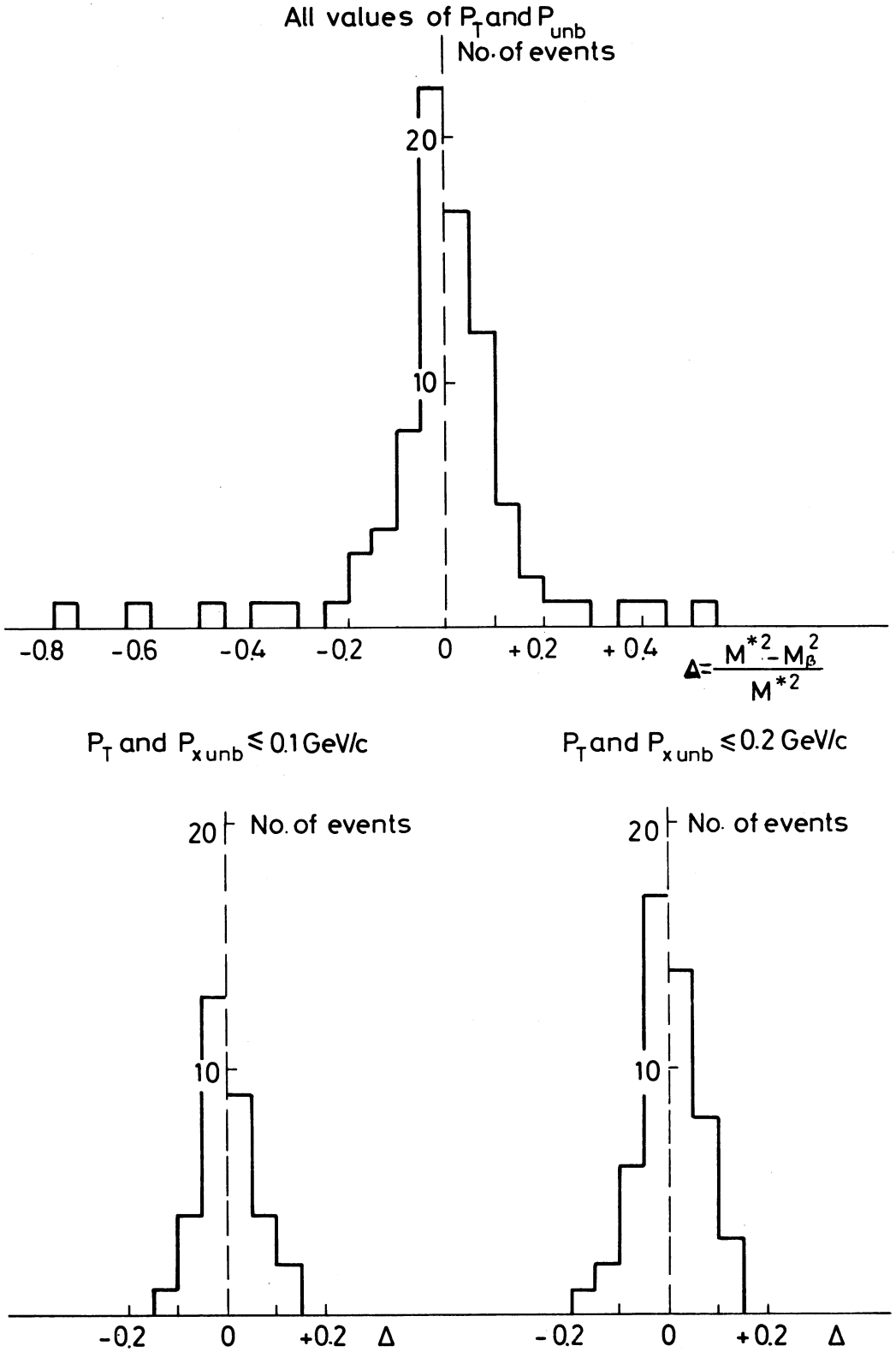

Fig. 9 : The function $\Delta = (M^{*2} - M_\beta^2)/M^{*2}$ for events on free protons for different cuts in P_T and $P_{x\,umb}$.